We are IntechOpen, the world's leading publisher of Open Access books Built by scientists, for scientists

4,800
Open access books available

122,000
International authors and editors

135M
Downloads

Our authors are among the

154
Countries delivered to

TOP 1%
most cited scientists

12.2%
Contributors from top 500 universities

CLARIVATE ANALYTICS BOOK CITATION INDEX INDEXED

WEB OF SCIENCE™

Selection of our books indexed in the Book Citation Index in Web of Science™ Core Collection (BKCI)

Interested in publishing with us?
Contact book.department@intechopen.com

Numbers displayed above are based on latest data collected.
For more information visit www.intechopen.com

15

Finite element analysis and Fracture in viscoelastic materials by Mθv integral-Part I: crack initiation

Rostand Moutou Pitti[1], Frédéric Dubois[2] and Mustapha Taazount[1]
[1]*Clermont Université, Blaise Pascal University, LaMI, EA 3867, BP 206, 63000 Clermont Ferrand, France*
[2]*Université de Limoges, GEMH, Centre Universitaire de Génie Civil, 19300 Egletons, France*

1. Introduction

Since few years, the finite element method appears a good tool for study the mechanical behaviour of mechanical or civil engineering structures submitted to complex high level of loading and environmental effects. Also, timber elements, like notched beams or joints, are generally subject to complex crack kinetics principally due to loading modes and orthotropic characters. In order to predict the initiation and the crack growth process, many numerical tools have been developed providing the mechanical field characterisation in the crack neighbourhood. Among them, it shown that energy methods are based on the use of unvarying integrals providing the evaluation of the energy release rate in accordance with a thermodynamic approach. However, some of these tools are mathematically limited to simple or global fracture modes for isotropic or orthotropic media.

This chapter book deals with the conservative law method (Noether, 1918), based on a non-dependent path integral providing the mixed mode separation with an expensive finite element discretisation. In the literature, Bui et al., (1985) has proposed a generalization of the J-integral (Rice, 1968) by separating displacement fields into a symmetric and antisymetric parts. This method is efficient but requires a symmetric mesh in the crack tip vicinity. Then, Chen & Shield, (1977) have developed the M-integral adapted to isotropic and elastic material, extended to orthotropic media by Moutou Pitti et al., (2007). This method allows the mixed mode fracture separation by using a virtual work principle introducing virtual fields in the integral definition. In order to introduce viscoelastic properties, the generalization of the M-integral for orthotropic material is investigated.

In order to develop a complete fracture mechanic algorithm, the first section reminds viscoelastic behaviour generalized for orthotropic configurations. The hereditary integral is transformed in an incremental formulation adapted for a finite element resolution. Since the fracture process is based on an energy balance, the numerical algorithm integrates the Helmholtz's free energy density concept.

The finite element implementation is presented in the second section. It is based on the incremental formulation treated by the virtual work principle. At each time increment, the subroutine enables us to access to the total mechanical field histories. An additional subroutine allows the time computation of the Helmholtz's free energy density requested to evaluate the energy release rate using invariant integrals.
The following part deals with a review of the thermodynamic formulation usually employed in the viscoelastic behaviour description and energetic balance. The main objective of this part is to recall different invariant integrals used in the energy release rate evaluation. More precisely, this section focus on the development of the Mθ-integral concept for, firstly, orthotropic media and, in the other hand, for viscoelastic behaviour. An additional incremental formulation is proposed in order to compute, step by step the energy release rate evolution versus time by separating open and shear mode parts.
Validations are proposed in the last section for cracked orthotropic and viscoelastic media. Based on a Compact Tension Shear geometry the algorithm validation is separated in two parts. Firstly, it is demonstrated the non-dependence property of the Mθ-integral. In a second time, numerical results are compared to analytic developments.

2. Viscoelastic formulation

The viscoelastic behavior is characterized by a time hereditary relationship between stresses and strains. A good understanding of the theory leads to present, firstly, a uniaxial development. Then, according to time evolutions of stress and strain scalar $\sigma(t)$ and $\varepsilon(t)$, respectively, the behavior law is described by a Boltzmann's integral :

$$\varepsilon(t) = \int_0^t J(t-\tau) \cdot \frac{\partial \sigma}{\partial \tau} d\tau \tag{1}$$

$J(t-\tau)$ is the time creep function in which t and τ are actual delayed times, respectively. Since several years, this formulation is implemented in the finite element method allowing a mechanical field definition and energy interpretations. The finite element implementation, of the hereditary integral (1), requests to develop memorization techniques for mechanical field history. In this context, Zienkiewicz et al. (1968) have been the first author proposing a direct time integration . However, this method necessitates storing the complete past histories of strain and stress tensors step by step inducing a very quick computer memory saturation. An alternative technique has been proposed consisting to replace the complex past history by a simplified form considering a past creep loading according to an equivalent creep time. If this method is a good compromise for to reduce the calculus price, the equivalent time doesn't be calculated for several creep functions according to anisotropic or orthotropic symmetries. In order to overcome these technical limits, specific incremental formulations have been developed. For isotropic media, Mansuero (1993) has proposed a pseudo uni axial technique using, firstly, a time incremental formulation based to a Prony's series representation of creep property and, in the other hand, a decomposition of the tridimensional behavior in terms of spherical and deviatoric parts. This method leads to transform a tridimensional behavior into two uni axial behaviors according to linear assumptions and the superposition principle. This method is quite efficient by replacing all past mechanical history by an only thermodynamic variable updated at each time

increment. Dubois et al. (1999) have proposed a generalization of this approach for anisotropic and orthotropic behaviors. In the same time, the energy balance requests to define the free energy evolution versus time. By using a spectral decomposition of of creep functions, suggested by Mandel (1966), the method enables us the definition of specific internal variables allowing specific free energy potential definition. For a good understanding of the approach let us present the method for a uni axial behavior; the three-dimensional generalization being developed later.

2.1 Incremental formulation

The spectral decomposition method consists on a creep function representation by a Prony's seri. According to specific compliance constants $J^{(0)}$ and $J^{(m)}$, the creep tensor admits the following form :

$$J(t) = J^{(0)} + \sum_{m=1}^{N} J^{(m)} \cdot (1 - e^{-\lambda^{(m)} \cdot t}) \tag{2}$$

in which $\lambda^{(m)}$ are functions of specific relaxation time. This representation is directly compatible with a generalized Kelvin Voigt model shown in Figure 1 composed by springs and dashpots according to stiffnesses $k^{(0)}$, $k^{(m)}$ and viscosities $\eta^{(m)}$, respectively, such as

$$J^{(0)} = \frac{1}{k^{(0)}},\ J^{(m)} = \frac{1}{k^{(m)}} \text{ and } \lambda^{(m)} = \frac{k^{(m)}}{\eta^{(m)}} \tag{3}$$

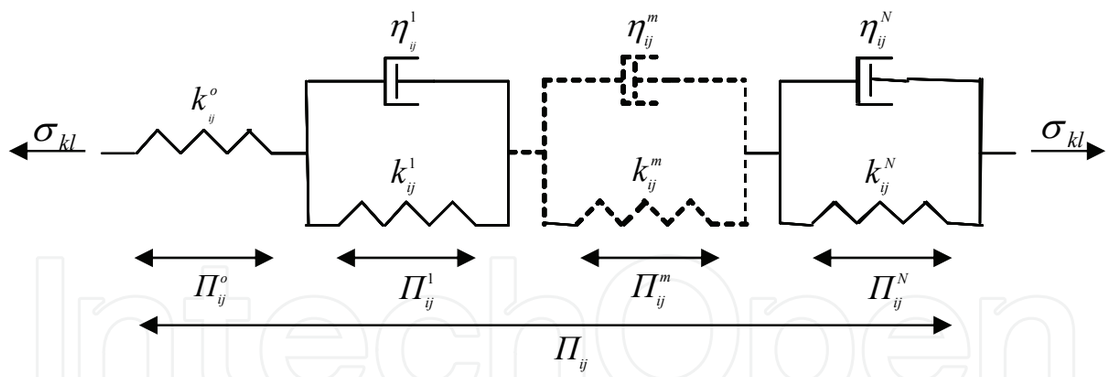

Fig. 1. Spectral decomposition of the strain tensor

Its form allows the strain separation such as

$$\varepsilon(t) = \varepsilon^{(0)} + \sum_{m=1}^{N} \varepsilon^{(m)} \tag{4}$$

$\varepsilon^{(0)}$ is the instantaneous and elastic strain. $\varepsilon^{(m)}$ is an differed strain part.

The time derivation of (4) is defined by

$$\frac{\partial \varepsilon(t)}{\partial t} = \frac{\partial \varepsilon^{(0)}}{\partial t} + \sum_{m=1}^{N} \frac{\partial \varepsilon^{(m)}}{\partial t} \tag{5}$$

The instantaneous strain rate is expressed by

$$\frac{\partial \varepsilon^{(0)}}{\partial t} = \frac{1}{k^{(0)}} \cdot \frac{\partial \sigma}{\partial t} \tag{6}$$

For the m[th] series term, the relationship between stress σ and strain $\varepsilon^{(m)}$ is governed by the following differential equation

$$\sigma = k^{(m)} \cdot \varepsilon^{(m)} + \eta^{(m)} \cdot \frac{\partial \varepsilon^{(m)}}{\partial t} \tag{7}$$

The time integration of equations (6) and (7) request a time discretization the incremental formulation requests a time discretization. If I indicates the full number of the considered time increment ($n \in \{1;...;I\}$), a time function $\alpha(t)$ is employed by supposing its linearity during the time step Δt_n ($\Delta t_n = t_n - t_{n-1}$). With this restriction, we consider, at the time t_n , following notations

$$\Delta\alpha_n = \alpha_n - \alpha_{n-1}\,,\ \frac{\partial \alpha_n}{\partial t} = \frac{\Delta\alpha_n}{\Delta t} \text{ and } \alpha_n = \alpha(t_n) \tag{8}$$

With the precedent expressions, equation (5) becomes, according to relation (6) :

$$\Delta\varepsilon_n = \frac{1}{k^{(0)}} \cdot \Delta\sigma_n + \sum_{m=1}^{N} \Delta\varepsilon_n^{(m)} \tag{9}$$

The problem is finally reduced to the evaluation of $\Delta\varepsilon_n^{(m)}$. In this case, the differential equation with second member and constant coefficient (7) is resolved by the constant variation method. We have finally

$$\Delta\varepsilon_n^{(m)} = \left(e^{-\lambda^{(m)} \cdot \Delta t_n} - 1\right) \cdot \varepsilon_{n-1}^{(m)} + \frac{1}{\eta^{(m)}} \cdot e^{-\lambda^{(m)} \cdot t_n} \cdot \int_{t_{n-1}}^{t_n} \sigma \cdot e^{-\lambda^{(m)} \cdot t}\, dt \tag{10}$$

However, supposing a linearity of σ between t_{n+1} *and* t_n :

$$\forall t \in \{t_{n-1}...t_n\},\ \sigma(t) = \sigma_{n-1} + \frac{t - t_{n-1}}{\Delta t_n} \cdot \Delta\sigma_n \tag{11}$$

By introducing the relation (11) in the formulation (10), we obtain

$$\begin{aligned} \Delta\varepsilon_n^{(m)} = &\left(e^{-\lambda^{(m)} \cdot \Delta t_n} - 1\right) \cdot \varepsilon_{n-1}^{(m)} + \left(\frac{1}{k^{(m)}} \cdot \left(1 - e^{-\lambda^{(m)} \cdot \Delta t_n}\right) \cdot \sigma_{n-1}\right) \\ &+ \frac{1}{k^{(m)}} \cdot \left(1 - \frac{1}{\lambda^{(m)} \cdot \Delta t_n} \cdot \left(1 - e^{-\lambda^{(m)} \cdot \Delta t_n}\right)\right) \cdot \Delta\sigma_n \end{aligned} \tag{12}$$

Finally, introducing expression (12) in (9), the strain increment can be written as follow

$$\Delta\varepsilon_n = \Psi_n \cdot \Delta\sigma_n + \tilde{\varepsilon}_{n-1} \tag{13}$$

Ψ_n represents the equivalent compliance traducing the effect of stress variation on the strain during the time increment Δt_n, defined by :

$$\Psi_n = \frac{1}{k^{(0)}} + \sum_{m=1}^{N} \frac{1}{k^{(m)}} \cdot \left(1 - \frac{1}{\lambda^{(m)} \cdot \Delta t_n} \cdot \left(1 - e^{-\lambda^{(m)} \cdot \Delta t_n} \right) \right) \tag{14}$$

$\tilde{\varepsilon}_{n-1}$ allows to update the material strain history. Actualized to each step of calculation, it's defined by

$$\tilde{\varepsilon}_{n-1} = \sum_{m=1}^{N} \left(\frac{1}{k^{(m)}} \cdot \left(1 - e^{-\lambda^{(m)} \cdot \Delta t_n} \right) \right) \cdot \sigma_{n-1} + \sum_{m=1}^{M} \left(e^{-\lambda^{(m)} \cdot \Delta t_n} - 1 \right) \cdot \varepsilon_{n-1}^{(m)} \tag{15}$$

2.2 3D generalizations

In order to generalize the uni axial incremental formulation, let us introduce the superposition principle considering pseudo several uni axial solicitations in which only the stress component σ_{kl} is non zero. Hence, the correspondent strain tensor Π_{ijkl} is separated in different parts (Ghazlan et al., 1995) (Dubois & Petit, 2005)

$$\Pi_{ijkl} = \Pi_{ijkl}^{(0)} + \sum_{m=1}^{N} \Pi_{ijkl}^{(m)} \quad avec \;\; m = \left(1; \ldots; N \right) \tag{16}$$

The behavior linearity allows to generalize the form (16) by employing the superposition principle such as

$$\varepsilon_{ij} = \sum_{k,l} \Pi_{ijkl} \;,\; \varepsilon_{ij}^{(0)} = \sum_{k,l} \Pi_{ijkl}^{(0)} \;\text{ and }\; \varepsilon_{ij}^{(m)} = \sum_{k,l} \Pi_{ijkl}^{(m)} \tag{17}$$

According to the generalized Kelvin Voigt model, the spectral decomposition of the creep tensor J_{ijkl} can be described by the association of springs $k_{ijkl}^{(p)}$ $\left(p \in \{0; 1; \ldots; N\} \right)$ and dashpots $\eta_{ijkl}^{(p)}$ $\left(m \in \{1; \ldots; N\} \right)$ such as

$$J_{ijkl}(t) = J_{ijkl}^{(0)} + \sum_{m=1}^{N} J_{ijkl}^{(m)} \cdot \left(1 - e^{-\lambda_{ijkl}^{(m)} \cdot t} \right) = \left[\frac{1}{k_{ijkl}^{(0)}} + \sum_{m=1}^{N} \frac{1}{k_{ijkl}^{(m)}} \cdot \left(1 - e^{-\lambda_{ijkl}^{(m)} \cdot t} \right) \right] \tag{18}$$

$$with \;\; \lambda_{ijkl}^{(m)} = \frac{k_{ijkl}^{(m)}}{\eta_{ijkl}^{(m)}}$$

In the time increment $\Delta t_n = t_n - t_{n-1}$ defined by the equation (8), by adding equation (13), the constitutive incremental low takes the following notation, without summation on the indices *kl* (Ghazlan et al. 1995)

$$\Delta\Pi_{ijkl}\left(t_n\right) = \Psi_{ijkl} \cdot \Delta\sigma_{kl}\left(t_n\right) + \tilde{\Pi}_{ijkl}\left(t_{n-1}\right) \tag{19}$$

$\Delta\Pi_{ijkl}(t_n)$ and $\Delta\sigma_{kl}(t_n)$ represent the increments of Π_{ijkl} and σ_{kl} respectively. $\tilde{\Pi}_{ijkl}(t_{n-1})$ is the pseudo stress at the time t_{n-1} witness of the influence of the strain past history in the various Kelvin Voigt cells. It takes the following notation:

$$\tilde{\Pi}_{ijkl}(t_{n-1}) = \sum_{m=1}^{N} \tilde{\Pi}_{ijkl}^{(m)}(t_{n-1})$$
$$with \quad \tilde{\Pi}_{ijkl}^{(m)}(t_{n-1}) = \left(e^{-\lambda_{ijkl}^{(m)}\cdot\Delta t_n} - 1\right) - \left[\frac{\sigma_{kl}(t_{n-1})}{k_{ijkl}^{(m)}} - \Pi_{ijkl}^{(m)}(t_{n-1})\right] \tag{20}$$

Ψ_{ijkl} is the component of the viscoelastic four order tensor compliance Ψ computing according to is actual uni axial form in the interval time Δt_n, it is noted by

$$\Psi_{ijkl} = \frac{1}{k_{ijkl}^{(0)}} + \sum_{m=1}^{N} \frac{1}{k_{ijkl}^{(m)}} \cdot \left(1 - \frac{1}{\lambda_{ijkl}^{(m)}\cdot\Delta t_n} \cdot \left(1 - e^{-\lambda_{ijkl}^{(m)}\cdot\Delta t_n}\right)\right) \tag{21}$$

The superposition principle allows obtaining the three-dimensional incremental law

$$\Delta\varepsilon_{ij}(t_n) = \Psi_{ijkl}\cdot\Delta\sigma_{kl}(t_n) + \tilde{\varepsilon}_{ij}(t_{n-1}) \tag{22}$$

$$\text{with } \tilde{\varepsilon}_{ij}(t_{n-1}) = \sum_{k,l} \tilde{\Pi}_{ijkl}(t_{n-1}) \;\; et \;\; \Delta\varepsilon_{ij}(t_n) = \sum_{k,l} \Delta\Pi_{ijkl}(t_n) \tag{23}$$

2.3 Helmholtz free energy density

The time fracture process in viscoelastic media is driven by energy approaches. More precisely, the energy balance puts in evidence two dissipation sources due to viscosity and crack lip separation. In these conditions, it's necessary to introduce an elastic released energy stored in the material which allows the justification of crack progression. According to specific energy definitions, this released energy is expressed as the Helmholtz free energy density F. According to notations introduced in (17) and (18), F takes the form defined as follow, (Moutou Pitti at al., 2007)

$$F = \frac{1}{2}\cdot k_{ijkl}^{(0)}\cdot\varepsilon_{ij}^{(0)}\cdot\varepsilon_{kl}^{(0)} + \sum_{m=1}^{N}\frac{1}{2}\cdot k_{ijkl}^{(m)}\cdot\varepsilon_{ij}^{(m)}\cdot\varepsilon_{kl}^{(m)} \tag{24}$$

$$\text{with } \varepsilon_{ij}^{(0)} = \frac{1}{k_{ijkl}^{(0)}}\cdot\sigma_{kl} \;\; et \;\; \varepsilon_{ij}^{(m)} = \int_0^t \frac{1}{k_{ijkl}^{(m)}}\cdot\left(1 - exp^{-\lambda_{ijkl}^{(m)}\cdot(t-\tau)}\right)\cdot\frac{\partial\sigma_{kl}}{\partial\tau}d\tau \tag{25}$$

The evaluation of *F*, equation (24), during each time step requires the determination of the strain increments of $\varepsilon_{ij}^{(0)}$ and $\varepsilon_{ij}^{(m)}$. In this case, by coupling the relation (25) with the incremental form (22), we obtain

$$\Delta\varepsilon_{ij}^{(0)}(t_n) = \frac{1}{k_{ijkl}^{(0)}}\cdot\Delta\sigma_{kl}(t_n) \quad et \;\; \Delta\varepsilon_{ij}^{(0)}(t_n) = \sum_{k,l}\Delta\Pi_{ijkl}^{(m)}(t_n) \tag{26}$$

$$\Delta\Pi_{ijkl}^{(m)}(t_n)=\left(e^{-\lambda_{ijkl}^{(m)}\cdot\Delta t_n}-1\right)\cdot\Pi_{ijkl}^{(m)}(t_{n-1})+\left(\frac{1}{k_{ijkl}^{(m)}}\cdot\left(1-e^{-\lambda_{ijkl}^{(m)}\cdot\Delta t_n}\right)\cdot\sigma_{kl}(t_{n-1})\right)$$
$$+\frac{1}{k_{ijkl}^{(m)}}\cdot\left(1-\frac{1}{\lambda_{ijkl}^{(m)}\cdot\Delta t_n}\cdot\left(1-e^{-\lambda_{ijkl}^{(m)}\cdot\Delta t_n}\right)\right)\cdot\Delta\sigma_{kl}(t_n) \quad (27)$$

3. Finite element implementation

3.1 Virtual work principle

The virtual work principle rests on an energy assessment with the free elastic energy density F and the work of the external efforts W_{ext} .In this case, supposing a virtual displacement kinematically admissible $\delta(\Delta\vec{u})$ and traducing a perturbation of a real field $\vec{u}$ in a balance configuration at the time t_{n-1}, the principle is traduced by

$$\delta F=\delta W_{ext} \quad (28)$$

Being given that the strain and the stress fields are known at the time t_{n-1}, the problem is reduced to the determination of mechanical fields at the next time $t_n=t_{n-1}+\Delta t_n$. The virtual displacement field $\delta(\Delta\vec{u})$ of components $\delta(\Delta u_i)$, around the configuration $\Omega(t)$, induces a virtual strain $\delta(\Delta\varepsilon_{ij})$ given by the Cauchy's tensor strain :

$$\delta\left(\Delta\varepsilon_{ij}\right)=\frac{1}{2}\cdot\left[\delta\left(\nabla(\Delta u)\right)+\delta\left(\nabla(\Delta u)^T\right)\right]$$
$$=\frac{1}{2}\cdot\left[\delta\left(\Delta u_{i,j}\right)+\delta\left(\Delta u_{j,i}\right)\right],\ et\ \delta\left(\Delta u_{i,j}\right)=\delta\left(\frac{\partial u_i}{\partial x_j}\right) \quad (29)$$

The free energy density and the sum of the external work efforts are respectively traduced by

$$\delta F(t_n)=\int_{\Omega(t_n)}\sigma_{ij}(t_n).\delta(\Delta\varepsilon_{ij})dV \quad (30)$$

$$\text{and } \delta W_{ext}(t_n)=\int_{\Omega(t_n)}f_{vi}(t_n).\delta(\Delta u_i)dV+\int_{\Omega_{f_S}(t_n)}f_{si}(t_n).\delta(\Delta u_i)dS \quad (31)$$

f_{vi} are the components of the volume forces in the domain Ω at the time t_n . f_{si} are the components of the imposed surface forces on the frontier of Ω_f during the same time lapse. Now, considering the following variable change

$$\sigma_{ij}(t_n)=\sigma_{ij}(t_{n-1})+\Delta\sigma_{ij}^n$$
$$f_{vi}(t_n)=f_{vi}(t_{n-1})+\Delta f_{vi}^n \quad (32)$$
$$f_{si}(t_n)=f_{si}(t_{n-1})+\Delta f_{si}^n$$

According to equations (28), (30), (31) and relations (32), we obtain

$$\int_{\Omega(t_n)}\left[\sigma_{ij}(t_{n-1})+\Delta\sigma_{ij}\right]\cdot\delta\left(\Delta\varepsilon_{ij}\right)dV=\int_{\Omega(t_n)}\left[f_{vi}(t_{n-1})+\Delta f_{vi}\right]\cdot\delta\left(\Delta u_i\right)dV + \int_{\Omega f_S(t_n)}\left[f_{si}(t_{n-1})+\Delta f_{si}\right]\cdot\delta\left(\Delta u_i\right)dS \tag{33}$$

The principle being checked at the time t_n and t_{n-1}, we obtain by recurrence the following expression

$$\int_{\Omega(t_n)}\Delta\sigma_{ij}\cdot\delta\left(\Delta\varepsilon_{ij}\right)dV=\int_{\Omega(t_n)}\Delta f_{vi}\cdot\delta\left(\Delta u_i\right)dV+\int_{\Omega f_S(t_n)}\Delta f_{si}\cdot\delta\left(\Delta u_i\right)dS \tag{34}$$

3.2 Finite element method

The relation (34) is reconsidered in a finite element discretization domain. The nodal unknown factors $\{\Delta u\}(t_n)$ are the values of the displacement field variation at the nodes of each under field. These values are computed from the real displacements fields $\Delta u(t_n)$, according to shape functions $N(x_1,x_2,x_3)$ characterizing the employed discretization elements

$$\Delta u(t_n)(x_1,x_2,x_3)=N(x_1,x_2,x_3)\cdot\{\Delta u\}(t_n) \tag{35}$$

The variation of the strain field vector $\{\Delta\varepsilon\}(t_n)$, computing at the integration points, is determined with the nodal displacements variations and the Jacobean matrix $[B]$:

$$\{\varepsilon\}(t_n)=[B]\cdot\{\Delta u\}(t_n) \tag{36}$$

By introducing the equations (35) and (36) in the equation (34), the incremental formulation law (22) becomes

$$\int_{\Omega(t_n)}[B]^T\cdot A\cdot[B]\cdot\{\Delta u\}(t_n)dV+\int_{\Omega(t_n)}[B]^T\cdot\{\tilde{\sigma}\}(t_{n-1})dV = \int_{\Omega f_S(t_n)}\{\Delta f_S\}(t_n)dS+\int_{\Omega(t_n)}\{\Delta f_v\}(t_n)dV \tag{37}$$

$$\text{with } A=\left(\Psi_{ijkl}\right)^{-1}(t_n) \text{ et } \tilde{\sigma}_{kl}(t_{n-1})=-\left(\Psi_{ijkl}\right)^{-1}(t_n)\cdot\tilde{\varepsilon}_{ijkl}(t_{n-1}) \tag{38}$$

$\{\tilde{\sigma}\}(t_{n-1})$ is the stress vector defined in the integration points of each calculated element starting from the stress field of components $\sigma_{kl}(t_{n-1})$. $\{\Delta f_v\}(t_n)$ and $\{\Delta f_s\}(t_n)$ are the volume and the surface nodal forces defined according to the forces of components $\Delta f_{vi}(t_n)$ and $\Delta f_{si}(t_n)$, respectively

$$\{\varepsilon\}(t_n)=[B]\cdot\{\Delta u\}(t_n) \tag{39}$$

$$\left\{\tilde{F}^p\right\}(t_{n-1})=-\int_{\Omega}B^T\cdot\Psi^p\cdot\left\{\tilde{\varepsilon}^p\right\}(t_{n-1})d\Omega \tag{40}$$

$$\left\{\Delta F^p_{ext}\right\}(t_n)=\int_{\Omega}\left\{\Delta f^p_s\right\}(t_n)dS+\int_{\Omega(t_n)}\left\{\Delta f^p_v\right\}(t_n)dV \tag{41}$$

K_T^p is the apparent rigidity tangent matrix in the time increment Δt_n . $\left\{\tilde{F}^p\right\}(t_{n-1})$ is the supplementary viscous load vector which represents the complete mechanical past history until the time t_{n-1} . $\left\{\Delta F_{ext}^p\right\}(t_n)$ is the increment of the external surface and volume nodal vector forces during the increment Δt_n . $\left\{\tilde{\varepsilon}^p\right\}(t_{n-1})$ is the strain history. At the end, the introduction of equations (39), (40) and (41) in the equality (37) conduces at the following finite element balance equation allowing the calculation of the nodal displacement vector increment $\left\{\Delta u^p\right\}(t_n)$

$$K_T^P \cdot \left\{\Delta u^p\right\}(t_n) = \left\{\Delta F_{ext}^p\right\}(t_n) + \left\{\tilde{F}^p\right\}(t_{n-1}) \tag{42}$$

4. Viscoelastic fracture mechanic

The main purpose of this part is the generalization and the modeling of the static M-integral, initially proposed by Chen & Shield, (1977), to orthotropic viscoelastic behavior. In this case, the surrounding integrals given by the energetic processes and the local approaches must be recalled. The algorithm is resolve in the finite element software Castem coupling the previous incremental formulation for viscoelastic behavior and the M-integral. The main topic is the calculation of the energy release rate evolution versus time by operating a mixed mode separation in viscoelastic and orthotropic media.

4.1 Energetic method

These methods provide the evaluation of the fracture parameters far from the defect introduced by the crack tip where the mechanical fields are largely disturbed by a strong singularity. The development of these tools is resulting from the conservative laws (Noether, 1971) and non dependant integral (Bui 2007).

J integral

In linear elasticity, for plane configurations and static cracks, energy required to create new crack surfaces is defined by Rice and its J-integral, (1968)

$$J = \int_{\Gamma} \left[F \cdot n_1 - \sigma_{ij} \cdot n_j \cdot \frac{\partial u_i}{\partial x_1} \right] d\Gamma \tag{43}$$

Γ is a curvilinear contour including the crack tip oriented by its normal vector $\vec{n}$ of components n_j ,Figure 2 (a).

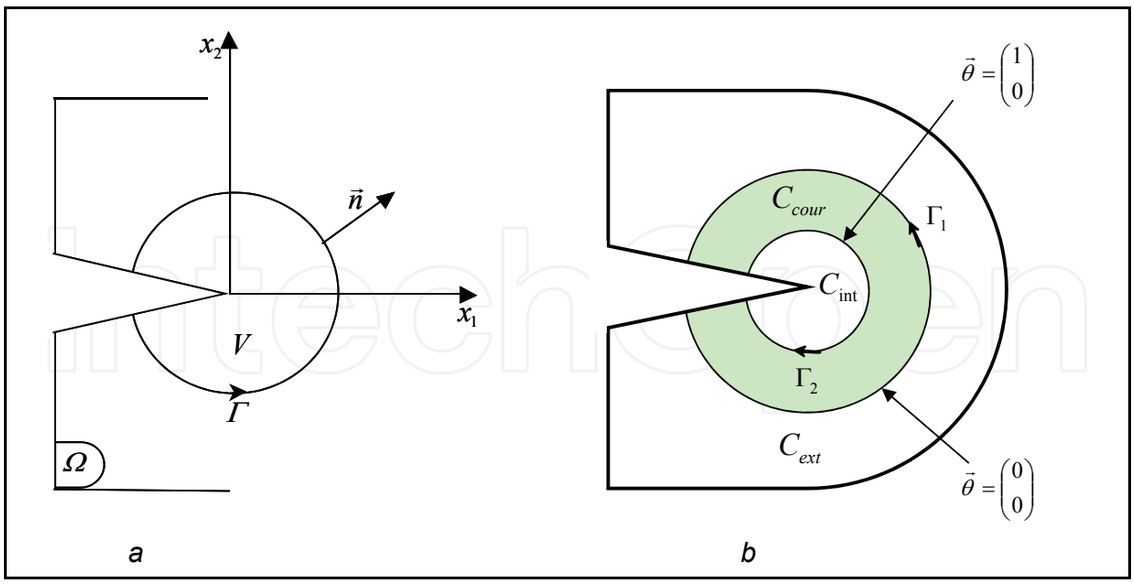

Fig. 2. a- Curvilinear line integral for the J-integral. b- θ field for the Gθ-integral

Gθ-integral

The J-integral, equation (43) is defined with a curvilinear line surrounding the crack tip. However, for the needs of implementation in a computer code and to ensure the fields continuity, it is preferable to define this expression on a surface integral in order to avoid the field's projections and numerical error sources. Destunyder et al. (1981, 1983) have defined a $\vec{\theta}$ vector field, continuous and differentiable allowing a virtual crown definition ($\theta_1 = 1$ inside the crown and $\theta_2 = 1$ outside it), Figure 2 (b). This vector field respects following proprieties:

- $\vec{\theta}$ is defined in the crack plan,
- $\vec{\theta}$ definition is in accordance with the crack growth direction,
- The support field $\vec{\theta}$ is concentrated in the crack tip neighborhood,

In fact, the contours Γ_1 and Γ_2 surrounding the crack tip can be defined. In we consider a crack growth in the x1 direction, the domain is divided in three parts, Figure 3 b (Moutou Pitti et al, 2007):

- In C_{int}, $\vec{\theta}$ is constant and takes the unitary value of $(1,0)$;
- In C_{ext}, the field $\vec{\theta}$ is zero $(0,0)$;
- In C_{cour}, the field $\vec{\theta}$ vary continuously of $\begin{pmatrix} 1 \\ 0 \end{pmatrix}$ to $\begin{pmatrix} 0 \\ 0 \end{pmatrix}$ according to a constant gradient.

Hence, the energy release rate can be expressed in the following term:

$$G\theta = \int_V \left[F \cdot \theta_{k,k} + \sigma_{ij} \cdot u_{i,k} \cdot \theta_k \right] dV \quad k \in \{1, 2\} \tag{44}$$

If integrals J and $G\theta$ provide to determine an invariant leading at the mechanical state in the crack vicinity, they operate a global energy calculation independently to the mixed mode fractures. For this reason, these integrals are employed only for pure opening or pure shear fracture modes.

Mθ-integrals

In order to separate mixed mode fracture, Chen and Shield, (1977) have proposed the following invariant integral

$$M = \frac{1}{2} \cdot \int_{\Gamma} \left[\sigma_{ij,1}^{(v)} \cdot u_i - \sigma_{ij}^{(u)} \cdot v_{i,1} \right] \cdot n_j d\Gamma \tag{45}$$

$\sigma_{ij}^{(u)}$ and $\sigma_{ij}^{(v)}$ are the real and virtual stresses field. The particularity of the M-integral lies in the joint combination of the real u and virtual v displacements fields kinematically acceptable. As the J-integral, M is defined on a curvilinear integration domain. In accordance with the previous part, we'd rather prefer a surface contour. In this case, the $M\theta$ integral (Moutou Pitti, 2007b) is defined for plane problems and takes the following form:

$$M\theta = \frac{1}{2} \cdot \int_{V} \left[\sigma_{ij}^{(u)} \cdot v_{i,k} - \sigma_{ij,k}^{(v)} \cdot u_i \right] \cdot \theta_{k,j} dV \tag{46}$$

For the orthotropic materials, virtual displacements fields v are given by Sih's singular form (Sih, 1974) for each fracture mode

$$\begin{aligned} v_1 = {} & 2 \cdot K_1^{(\sigma)} \cdot \sqrt{\frac{r}{2 \cdot \pi}} \cdot \Re e \left[\frac{1}{s_1 - s_2} \cdot \left(p_2 \cdot s_1 \cdot \sqrt{\rho_2} - p_1 \cdot s_2 \cdot \sqrt{\rho_1} \right) \right] \\ & + 2 \cdot K_2^{(\sigma)} \cdot \sqrt{\frac{r}{2 \cdot \pi}} \cdot \Re e \left[\frac{1}{s_1 - s_2} \cdot \left(p_2 \cdot \sqrt{\rho_2} - p_1 \cdot \sqrt{\rho_1} \right) \right] \end{aligned} \tag{47}$$

$$\begin{aligned} v_2 = {} & 2 \cdot K_1^{(\sigma)} \cdot \sqrt{\frac{r}{2 \cdot \pi}} \cdot \Re e \left[\frac{1}{s_1 - s_2} \cdot \left(q_2 \cdot s_1 \cdot \sqrt{\rho_2} - q_1 \cdot s_2 \cdot \sqrt{\rho_1} \right) \right] \\ & + 2 \cdot K_2^{(\sigma)} \cdot \sqrt{\frac{r}{2 \cdot \pi}} \cdot \Re e \left[\frac{1}{s_1 - s_2} \cdot \left(q_2 \cdot \sqrt{\rho_2} - q_1 \cdot \sqrt{\rho_1} \right) \right] \end{aligned}$$

$$\text{with } \rho_j = cos(\theta) + i \cdot s_j \cdot sin(\theta) \quad avec\, j \in \{1;2\} \tag{48}$$

$$\text{and } p_j = S_{11} \cdot {s_j}^2 + S_{12} \quad et \quad q_j = \frac{S_{22}}{s_j} + S_{12} \tag{49}$$

s_j are roots of the following characteristic equation:

$$S_{11} \cdot {s_\beta}^4 + \left(2 \cdot S_{12} + S_{33} \right) \cdot {s_\beta}^2 + S_{22} = 0 \tag{50}$$

S_{11}, S_{12}, S_{22}, S_{33} designate components of the compliance tensor in an orthotropic symmetry.

Physical interpretation of Mθ integral

For real and virtual kinematically admissible displacement fields u and v, respectively, Dubois et a, 1999 have shown the following physical interpretation:

$$M\left(u,u\right)=J=G \tag{51}$$

In linear elasticity, the following physical interpretation can be easily demonstrated

$$M\theta\left(u,v\right)=C_1\cdot\frac{{}^{u}K_I\cdot{}^{v}K_I}{8}+C_2\cdot\frac{{}^{u}K_{II}\cdot{}^{v}K_{II}}{8} \tag{52}$$

C_1 and C_2 are the reduced elastic compliances in opening and shear mode allowing the estimation of elastic response between local stress field in the crack tip vicinity and the crack opening. For an orthotropic symmetry, their forms are defined by Valentin et al. (1989)

$$C_1=4\cdot\Re e\left[\frac{i\cdot\left(q_2\cdot s_1-q_1\cdot s_2\right)}{s_1-s_2}\right]\ \ and\ \ C_2=4\cdot\Re e\left[\frac{i\cdot\left(p_2-p_1\right)}{s_1-s_2}\right] \tag{53}$$

In order to express the real stress intensity factors ${}^{u}K_I$ and ${}^{u}K_{II}$, the perfect mixed mod separation is obtain by implementing two different calculations of the $M\theta\left(u,v\right)$ integral. In this case, judicious values for the virtual stress intensity factor ${}^{v}K_I$ and ${}^{v}K_{II}$ as chosen (Moutou Pitti 2008)

$${}^{u}K_I=8\cdot\frac{M\left({}^{v}K_I=1\,,\,{}^{v}K_{II}=0\right)}{C_I}\quad and\quad {}^{u}K_{II}=8\cdot\frac{M\left({}^{v}K_I=0\,,\,{}^{v}K_{II}=1\right)}{C_{II}} \tag{54}$$

4.2 Generalization to viscoelastic behavior

The introduction of the M-integral in a viscoelastic behavior integrates the similitude between the generalized Kelvin Voigt model shown in Figure 1 and the Helmholtz free energy density which is a energy summation on different elastic elements, expression (24). In this case, the equation (45) has generalized as follow (Moutou Pitti et al 2007; Moutou Pitti, 2008)

$$M_v^{(k)}=\frac{1}{2}\cdot\int_{\Gamma}\left[\sigma_{ij,1}^{(k)}\left(v\right)\cdot u_i^{(k)}-\sigma_{ij}^{(k)}\left(u\right)\cdot v_{i,1}^{(k)}\right]\cdot n_j d\Gamma\quad avec\quad k=\left(0,1,...,N\right) \tag{55}$$

$\sigma_{ij}^{(k)}\left(u\right)$ and $\sigma_{ij}^{(k)}\left(v\right)$ indicate the real and virtual stresses in the kth spring, respectively. u_i^k and v_i^k are real and virtual displacements of this spring induced by real and virtual elastic stresses. According to the generalization of the expression (46), we obtain the Mθv-integral for a viscoelastic field

$$M\theta_v^{(k)}=\frac{1}{2}\cdot\int_{V}\left[\sigma_{ij}^{(k)}\left(u\right)\cdot u_i^{(k)}-\sigma_{ij,k}^{(k)}\left(v\right)\cdot v_{i,k}^{(k)}\right]\cdot\theta_{k,j}dV\quad avec\quad k=\left(0,1,...,N\right) \tag{56}$$

With the same way of equations (52) and (54), we obtain successively :

$$M\theta_v^{(k)} = C_1^{(k)} \cdot \frac{{}^{u}K_I^{(k)} \cdot {}^{v}K_I^{(k)}}{8} + C_2^{(k)} \cdot \frac{{}^{u}K_{II}^{(k)} \cdot {}^{v}K_{II}^{(k)}}{8} \tag{57}$$

$${}^{u}K_I^{(k)} = 8 \cdot \frac{M\theta_v^{(k)}\left({}^{v}K_I^{(k)} = 1\,,\ {}^{v}K_{II}^{(k)} = 0\right)}{C_1^{(k)}}$$

and (58)

$${}^{u}K_{II} = 8 \cdot \frac{M\theta_v^{(k)}\left({}^{v}K_I^{(k)} = 0\,,\ {}^{v}K_{II}^{(k)} = 1\right)}{C_2^{(k)}}$$

${}^{v}K_I^{(k)}$ and ${}^{v}K_{II}^{(k)}$ are virtual stress intensity factors characterizing the stress field induced respectively by $v_1^{(k)}$ and $v_2^{(k)}$ for the k[th] spring. In the same case of equations (47), (48), (49) and (50), these virtual displacement are rewritten as

$$v_1^{(k)} = 2 \cdot {}^{v}K_I^{(k)} \cdot \sqrt{\frac{r}{2\cdot\pi}} \cdot \Re e\left[\frac{1}{s_1^{(k)} - s_2^{(k)}} \cdot \left(p_2^{(k)} \cdot s_1^{(k)} \cdot \sqrt{\rho_2^{(k)}} - p_1^{(k)} \cdot s_2^{(k)} \cdot \sqrt{\rho_1^{(k)}}\right)\right]$$
$$+ 2 \cdot {}^{v}K_{II}^{(k)} \cdot \sqrt{\frac{r}{2\cdot\pi}} \cdot \Re e\left[\frac{1}{s_1^{(k)} - s_2^{(k)}} \cdot \left(p_2^{(k)} \cdot \sqrt{\rho_2^{(k)}} - p_1^{(k)} \cdot \sqrt{1^{(k)}}\right)\right] \tag{59}$$

$$v_2^{(k)} = 2 \cdot {}^{v}K_I^{(k)} \cdot \sqrt{\frac{r}{2\cdot\pi}} \cdot \Re e\left[\frac{1}{s_1^{(k)} - s_2^{(k)}} \cdot \left(q_2^{(k)} \cdot s_1^{(k)} \cdot \sqrt{\rho_2^{(k)}} - q_1^{(k)} \cdot s_2^{(k)} \cdot \sqrt{\rho_1^{(k)}}\right)\right]$$
$$+ 2 \cdot {}^{v}K_{II}^{(k)} \cdot \sqrt{\frac{r}{2\cdot\pi}} \cdot \Re e\left[\frac{1}{s_1^{(k)} - s_2^{(k)}} \cdot \left(q_2^{(k)} \cdot \sqrt{\rho_2^{(k)}} - q_1^{(k)} \cdot \sqrt{\rho_1^{(k)}}\right)\right]$$

$$\rho_j^{(k)} = cos(\theta) + i \cdot s_j^{(k)} \cdot sin(\theta) \quad with\, j \in \{1;2\} \quad and$$

$$\text{with } p_j^{(k)} = S_{11}^{(k)} \cdot \left(s_j^{(k)}\right)^2 + \left(S_{12}^{(k)}\right)^2 \ and\ q_j^{(k)} = \frac{S_{22}^{(k)}}{s_j^{(k)}} + S_{12}^{(k)} \cdot s_j^{(k)} \tag{60}$$

$$S_{11}^{(k)} \cdot \left(s_j^{(k)}\right)^4 + \left(2 \cdot S_{12}^{(k)} + S_{33}^{(k)}\right) \cdot \left(s_j^{(k)}\right)^2 + S_{22}^{(k)} = 0$$

By combining equations (57) and (58), we obtain the following viscoelastic energy release rate

$$G_v^{(k)} = {}^{1}G_v^{(k)} + {}^{2}G_v^{(k)} = C_1^{(k)} \cdot \frac{\left({}^{u}K_I^{(k)}\right)^2}{8} + C_2^{(k)} \cdot \frac{\left({}^{u}K_{II}^{(k)}\right)^2}{8} \tag{61}$$

5. Local mechanical fields

In order to define the mechanical fields at the crack tip, Chazal & Dubois, (2001) and Dubois et al, (2002) have proposed, for plane problems, two viscoelastic stress intensity factors ${}^{u}K_{\alpha}^{(\sigma)}\left(\alpha=\{1;2\}\right)$ and two viscoelastic opening displacement intensity factors such as, (Figure 3)

$$\sigma_{ij}=\frac{1}{\sqrt{2\cdot\pi\cdot r}}\cdot {}^{u}K_{\alpha}^{(\sigma)}\cdot f_{ij\alpha}(\theta) \tag{62}$$

$$\left[u_{\alpha}\right]=\sqrt{\frac{r}{2\cdot\pi}}\cdot {}^{u}K_{\alpha}^{(\varepsilon)} \tag{63}$$

$f_{ij\alpha}\left(\theta\right)$ is a function which depends on the local properties of material (Irwin, 1957). $\left[u_{\alpha}\right]$ are the components of the crack opening displacement which designates the relative displacement vector of crack lips. Considering the Boltzmann integral (1) into expressions (62) and (63), the relationship between stress and crack opening intensity factors takes the following form (Dubois et al. 1999)

$${}^{u}K_{\alpha}^{(\varepsilon)}=\int_{0}^{t}C_{\alpha}\left(t-\tau\right)\cdot\frac{\partial {}^{u}K_{\alpha}^{(\sigma)}}{\partial\tau}d\tau \tag{64}$$

C_{α} is the viscoelastic compliance function for α mode and takes a similar creep function form in accord with a generalized Kelvin Voigt model, Figure 3 :

$$C_{\alpha}\left(t\right)=\frac{1}{k_{\alpha}^{(0)}}+\sum_{m=1}^{N}\frac{1}{k_{\alpha}^{(0)}}\cdot\left(1-exp^{-\lambda_{\alpha}^{(m)}\cdot t}\right)\quad avec\quad \lambda_{\alpha}^{(m)}=\frac{k_{\alpha}^{(m)}}{\eta_{\alpha}^{(m)}} \tag{65}$$

$k_{\alpha}^{(p)}\ \left(p\in\{0;1;\ldots;N\}\right)$ and $\eta_{\alpha}^{(m)}\ \left(m\in\{1;\ldots;N\}\right)$ are the contribution of tensor components $k_{ijkl}^{(p)}$ and $\eta_{ijkl}^{(p)}$ respectively. $\frac{1}{k_{\alpha}^{(0)}}$ are the reduced elastic compliance defined by the equation (53). With a strain analogy, equation (4) allows a partition of the crack opening intensity factor traduced by

$${}^{u}K_{\alpha}^{(\varepsilon)}={}^{u}K_{\alpha}^{(0)}+\sum_{m=1}^{N}{}^{u}K_{\alpha}^{(m)} \tag{66}$$

with

$$\begin{aligned}&{}^{u}K_{\alpha}^{(0)}=\frac{1}{k_{\alpha}^{(0)}}\cdot {}^{u}K_{\alpha}^{(\sigma)}\quad et\\ &and\quad {}^{u}K_{\alpha}^{(p)}=\int_{0}^{t}\frac{1}{k_{\alpha}^{(p)}}\cdot\left(1-exp^{-\lambda_{\alpha}^{(p)}\cdot(t-\tau)}\right)\cdot\frac{\partial {}^{u}K_{\alpha}^{(\sigma)}}{\partial\tau}d\tau\end{aligned} \tag{67}$$

If we take into account the definition of the Helmholtz energy density of introduced (Staverman & Schwarzl 1952), the viscoelastic energy release rate, traduced by the local proprieties at the crack tip, is (Moutou Pitti et al, 2007)

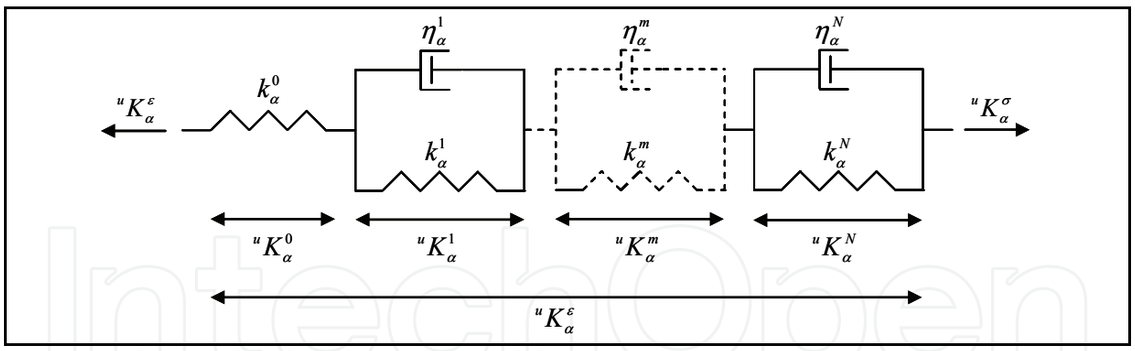

Fig. 3. Local generalized Kelvin Voigt model

$$ {}^{\alpha}G_v(t) = \frac{1}{8}\cdot\int_0^t\int_0^t \left[2\cdot C_\alpha(t-\tau) - C_\alpha(2\cdot t-\tau-\beta)\right]\cdot\frac{\partial\,{}^uK_\alpha^{(\sigma)}}{\partial\tau}\frac{\partial\,{}^uK_\alpha^{(\sigma)}}{\partial\beta}\,d\tau\,d\beta \tag{68} $$

By combining Equations (61), (67) and (68), the partition of viscoelastic energy release rate ${}^{\alpha}G_v$ is given by

$$ {}^{\alpha}G_v = {}^{\alpha}G_v^{(0)} + \sum_{m=1}^{N} {}^{\alpha}G_v^{(m)} \tag{69} $$

$$ \text{with } G_v^{(p)} = \frac{1}{8}\cdot\frac{1}{k_\alpha^{(p)}}\cdot\left[{}^uK_\alpha^{(p)}\right]^2 \quad \textit{and} \quad {}^{\alpha}G_v^{(0)} = \frac{1}{8}\cdot\frac{1}{k_\alpha^{(0)}}\cdot\left[{}^uK_\alpha^{(0)}\right]^2 \tag{70} $$

5.2 Numerical algorithm

This section deals with the numerical procedure implemented in the finite software Castem. The uncoupling between the viscoelastic incremental formulation and the fracture mode process is proposed. In the general subroutine, the algorithm computing the virtual mechanical fields is added (Moutou Pitti et al. 2007). In order to explain this algorithm, we suppose that mechanical fields are known at time t_{n-1} and we have fixed the time increment Δt_n. All properties of viscoelastic material are experimentally defined (Dubois et al. 2001). The different steps of the algorithm are defined as follow, Figure 4

- The tensor Ψ, expression (21) is computed, and the global tangent rigidity matrix K_T is deduced.
- The supplementary viscoelastic load field $\left\{F^p\right\}(t_{n-1})$ is determined with expression (40).
- By introducing the exterior vector force $\{\Delta F_{ext}\}(t_n)$, equation (41), in the equation (42), the nodal displacement incremental $\{\Delta u\}(t_n)$ and the different mechanical fields $\{u\}(t_n)$, $\{\varepsilon\}(t_n)$ *et* $\{\sigma\}(t_n)$ are obtained. The compliance tensor Ψ^P is

introduced according to the proprieties k_{ijkl}^{p} of the material. After, the strain tensor $\left\{\varepsilon^{p}\right\}(t_n)$ is calculated and the viscoelastic tangent matrix K_T^p is obtained.

- The elastic tress tensor $\left\{\sigma^{(p)}\right\}(t_n)$ and the nodal force vector $\left\{F^{(p)}\right\}(t_n)$ are calculated. For each model spring, nodal displacement vector $\left\{u^{(p)}\right\}$ are deduced of the following finite element balance equation $K_T^p \cdot \left\{u^{(p)}\right\}(t_n) = \left\{u^{(p)}\right\}(t_n)$
- Finally, the stress intensity factor ${}^{u}K_{\alpha}^{(p)}$ and the energy release rate ${}^{\alpha}G\theta_{v}^{(p)}$ evaluation necessitate the virtual displacement $v_{\alpha}^{(p)}$, expression (59), the viscoelastic compliance $C_{\alpha}^{(p)}$, and virtual stress tensor ${}^{\alpha}\sigma_{virt}^{(p)}$. ${}^{u}K_{\alpha}^{(p)}$ and ${}^{\alpha}G\theta_{v}^{(p)}$ are given by the $M\theta$ subroutine. At the end, a final summation on ${}^{\alpha}G\theta_{v}^{(p)}$ gives the global energy release rate for each fracture mode ${}^{\alpha}G_{v}$:

$$ {}^{\alpha}G_{v} = {}^{\alpha}G\theta_{v}^{(0)} + \sum_{m=1}^{N} {}^{\alpha}G\theta_{v}^{(m)} = \sum_{m=1}^{N} {}^{\alpha}G\theta_{v}^{(p)} \tag{71} $$

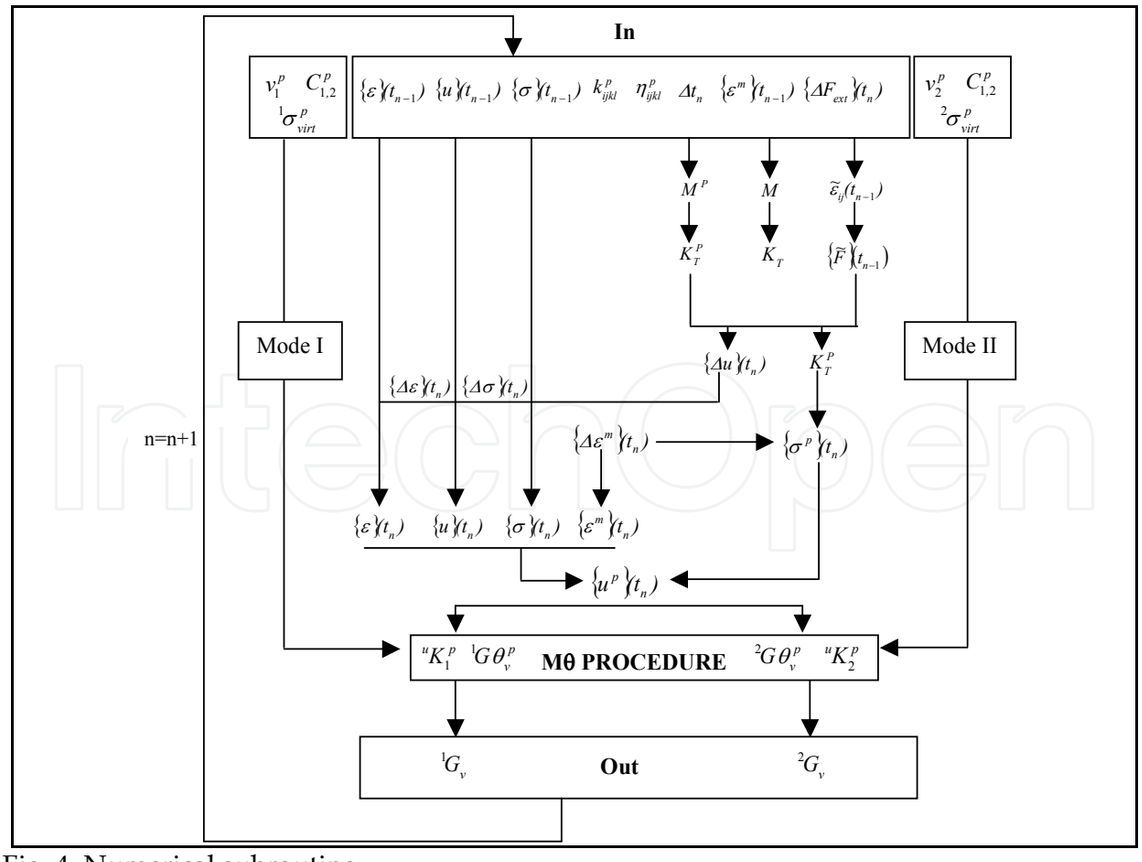

Fig. 4. Numerical subroutine

6. Numerical validation

6.1 Compact Tension Shear specimen

The CTS geometry has been initially developed by Richard, (1981) in order to separate fracture modes in isotropic materials. Valentin & Caumes (1989) have adapted this specimen to orthotropic material as wood. On Figure 5, the initial crack length chosen is 25 mm. The external load is a unitary loading applied to a perfect rigid steel arm (which presents a large crack growth zone), Figure 6. Points A_α *and* B_α *with* $\alpha \in (1...7)$ are holes where forces can be applied with the angle β oriented according to the trigonometrically direction for different mixed mode ratios. The simple opening mode is obtained by applying opposite forces in A_1 and B_1 with $\beta = 0°$. The loading $\beta = 90°$, in A_7 and B_7 corresponds to a simple shear mode configuration. Intermediary positions induce different mixed mode ratios.

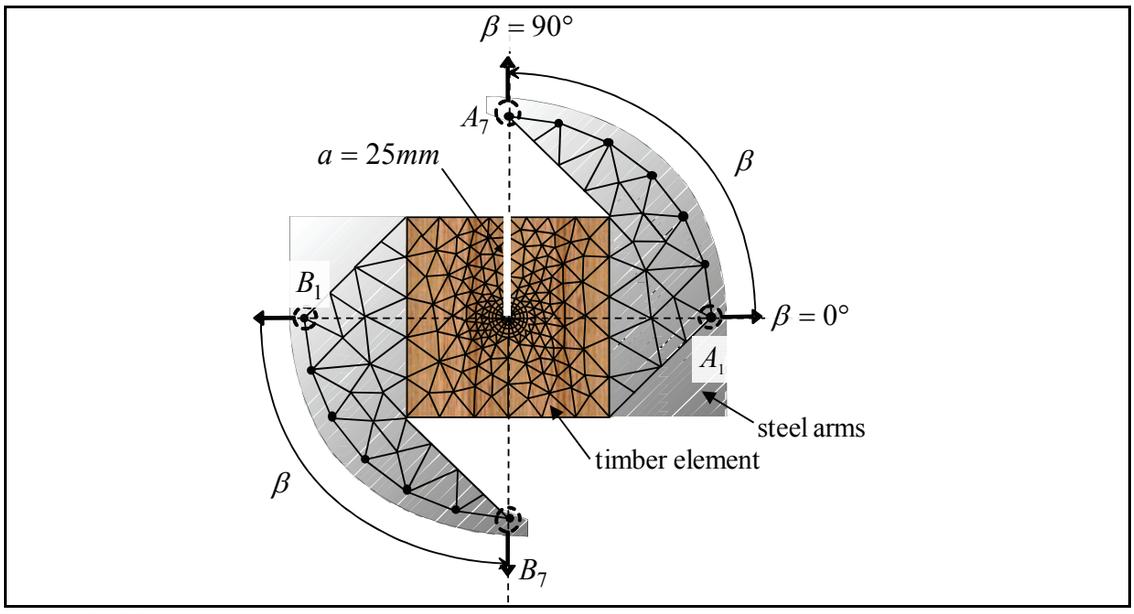

Fig. 5. CTS Specimen

In order to simplify the analytical development in the temporal field, the creep tensor is chosen as a proportional time function such as

$$[J](t) = \frac{1}{E_L(t)} \cdot [C_0] \tag{72}$$

C_0 is a constant and unit compliance tensor composed by a unity elastic modulus and a constant Poisson coefficient of 0,4. $E_L(t)$ designates the tangent modulus for the longitudinal direction. In this context, the creep properties are given in terms of creep function by interpolating $1/E_L(t)$ with six Kelvin Voigt cells, Figure 6.

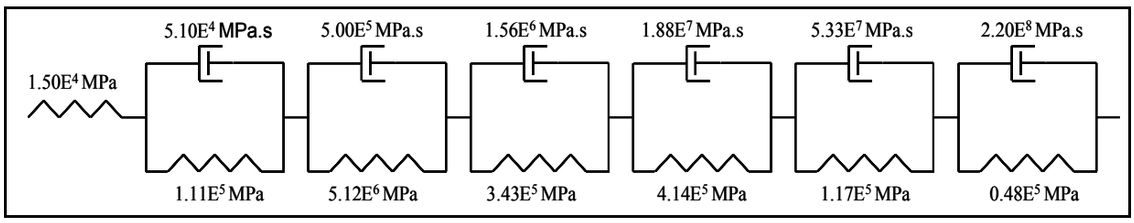

Fig. 6. Spectral decomposition of $1/E_L(t)$ (Moutou Pitti, 2008)

$1/E_L(t)$ takes the following analytic form :

$$\frac{1}{E_L(t)} = \frac{1}{E_L(0)} \cdot \left[\begin{array}{l} 1 + \frac{1}{74,3} \cdot \left(1 - exp\left(-\frac{74,3}{3,37} \cdot t \right) \right) + \frac{1}{74,4} \cdot \left(1 - exp\left(-\frac{74,4}{33,37} \cdot t \right) \right) \\ + \frac{1}{22,9} \cdot \left(1 - exp\left(-\frac{22,9}{104,09} \cdot t \right) \right) + \frac{1}{27,6} \cdot \left(1 - exp\left(-\frac{27,6}{1251} \cdot t \right) \right) \\ + \frac{1}{7,83} \cdot \left(1 - exp\left(-\frac{7,83}{3554} \cdot t \right) \right) + \frac{1}{3,23} \cdot \left(1 - exp\left(-\frac{3,23}{14660} \cdot t \right) \right) \end{array} \right] \tag{73}$$

in which $E_L(0) = 15000MPa$ is the elastic longitudinal Young modulus for longitudinal direction. C_0 admits the definition for plane configurations

$$C_0 = \begin{bmatrix} 1 & -\upsilon & 0 \\ -\upsilon & \frac{E_L(t)}{E_R} & 0 \\ 0 & 0 & \frac{E_L(t)}{G_{LR}} \end{bmatrix} \tag{74}$$

$E_R = 600MPa$ and $G_{LR} = 700MPa$ are the transverse and shear modulus, respectively.

6.2 Displacement fields and meshes

The linear triangular elements with 3 nodes were used. If the thickness of the specimen is very low compared to two other dimensions, the modeling in plan stress is used. Like boundary conditions, the crack tip displacement is blocked. It is the same for the lower part of the wood specimen. On the line of cracking, displacements along the axis x are prevented. In order to have stable results, a radiant mesh is used around the crack tip. Figure 7 illustrates the virtual finite element deformation in opening and shear modes.

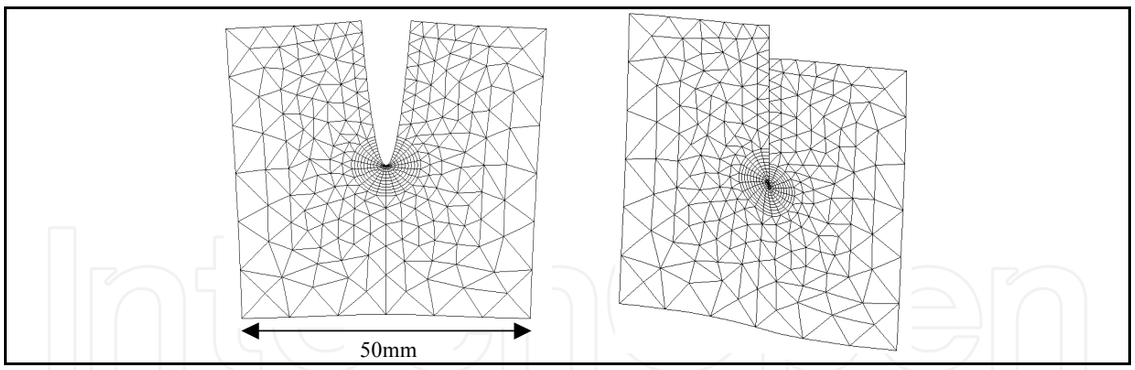

Fig. 7. Virtual displacements in opening and shear modes

Figure 8 (a) presents the detail of the radiant mesh around the crack tip on which the component θ_L of the field $\vec{\theta}$ is visualized, Figure 8 (b).

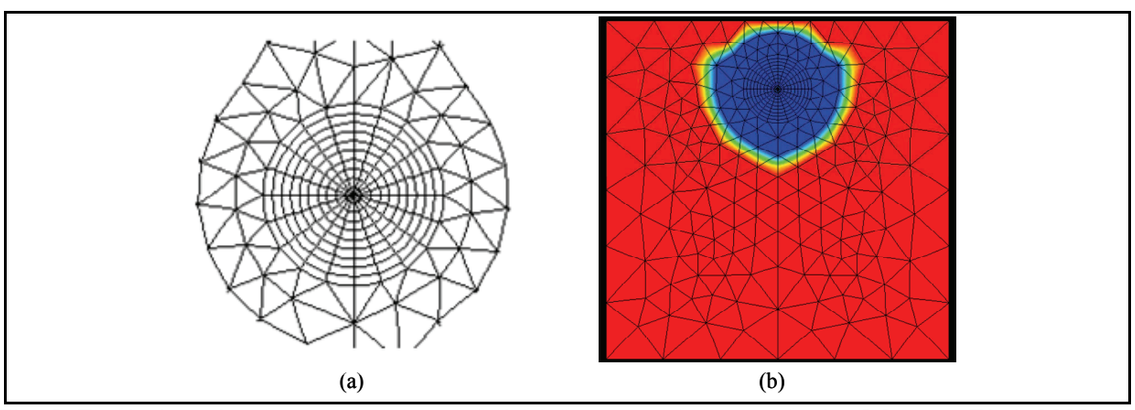

Fig. 8. Radiating circular mesh (a) and θ field (b) around the crack tip (Moutou Pitti, 2008)

6.3 Path independence domain

The independence path integral is checked by representing the various variations of the energy release rate versus each crown illustrating the size of the field $\vec{\theta}$. Five crowns noted and numbered C0 to C8, Figure 9, were tested.

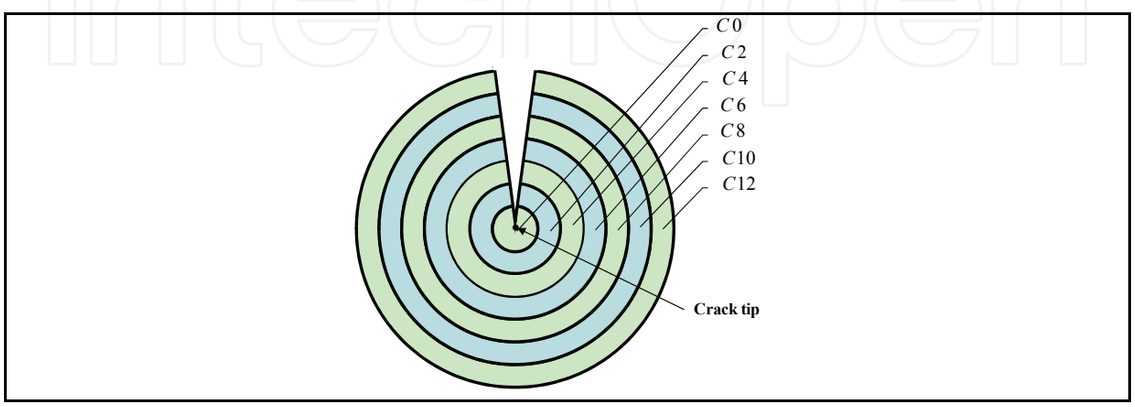

Fig. 9. Integration crowns

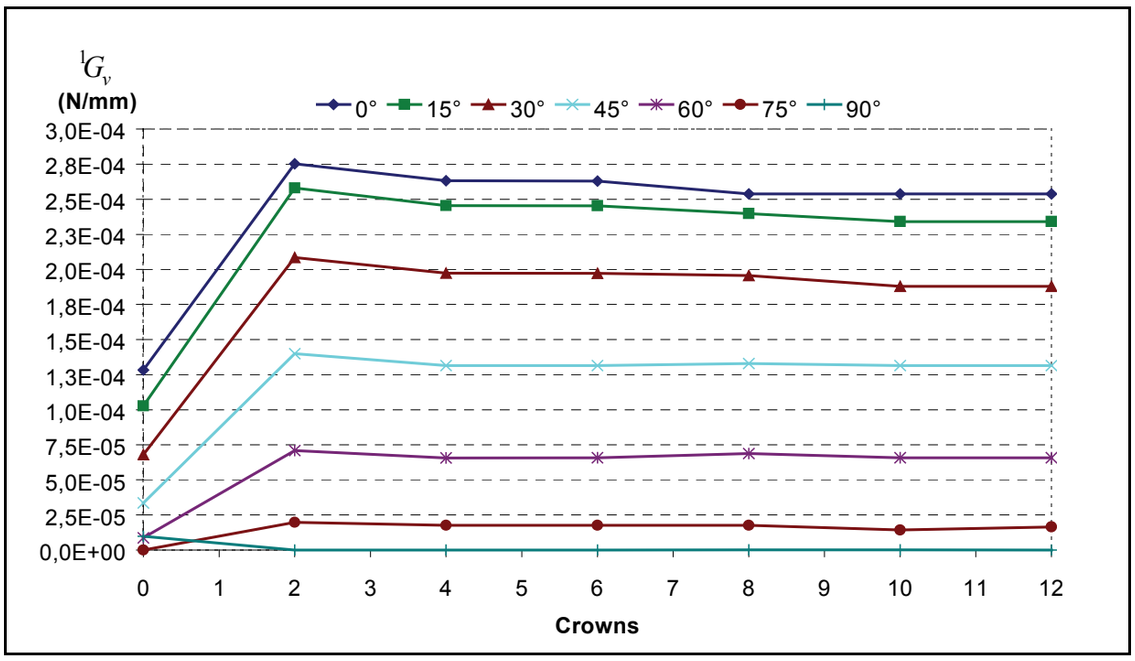

Fig. 10. Path independence domain ^1G_v (opening mode) versus orientation angle β

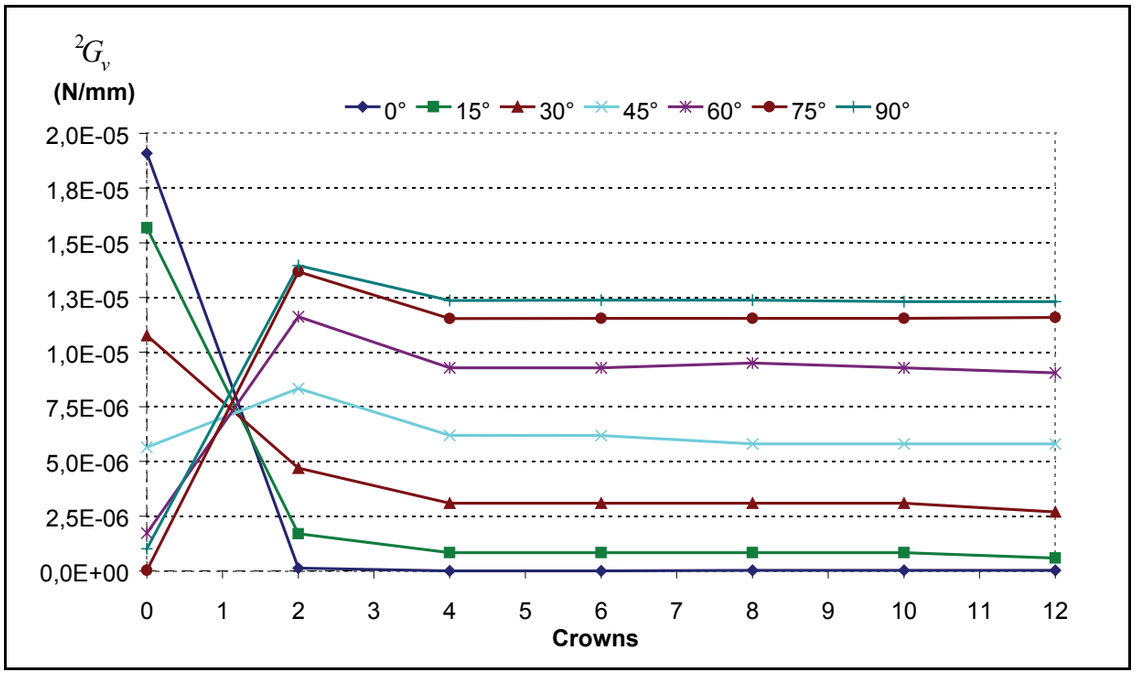

Fig. 11. Path independence domain ^2G_v (shear mode) versus angle orientation β

Figures 9 and 10 show the energy release rate evolution in mode I and mode II versus the loading orientation and the various integration crowns, for a unit loading. Results were obtained after a creep time of 720 seconds. The constancy of the viscoelastic energy release rate (less of fluctuation) versus crowns in mode I, mode II and in mixed modes (share of

mode I and leaves mode II, respectively) is noted. These observations validate the path independence domain and the stability of results ensured by the model. However, the singularity of the mechanical fields at the crack tip causes field disturbance integration around the crack area (first two crowns), and this, for the two fracture modes.

6.3 Comparison of analytical and numerical solution

In order to validate the viscoelastic procedure, Results given by the numerical solution are compared with the analytical calculus resulting from the isothermal Helmholtz free energy density, equations (68). From relation (65), the viscoelastic creep tensor in mode I and mode II, respectively, takes the following form:

$$C_1(t) = C_1^{(0)} \cdot f(t) = 7,35 \cdot 10^{-3} \cdot f(t) \tag{75}$$

$$C_2(t) = C_2^{(0)} \cdot f(t) = 1,47 \cdot 10^{-3} \cdot f(t) \tag{76}$$

$C_1^{(0)}$ and $C_2^{(0)}$ represent the reduced elastic compliances, equations (53). The time creep function $f(t)$ admits an similarly form of (73) such as

$$f(t) = \left[\begin{array}{l} 1 + \frac{1}{74,3} \cdot \left(1 - exp^{\left(-\frac{74,3}{3,37} \cdot t \right)} \right) + \frac{1}{74,4} \cdot \left(1 - exp^{\left(-\frac{74,4}{33,37} \cdot t \right)} \right) \\ + \frac{1}{22,9} \cdot \left(1 - exp^{\left(-\frac{22,9}{104,09} \cdot t \right)} \right) + \frac{1}{27,6} \cdot \left(1 - exp^{\left(-\frac{27,6}{1251} \cdot t \right)} \right) \\ + \frac{1}{7,83} \cdot \left(1 - exp^{\left(-\frac{7,83}{3554} \cdot t \right)} \right) + \frac{1}{3,23} \cdot \left(1 - exp^{\left(-\frac{3,23}{14660} \cdot t \right)} \right) \end{array} \right] \tag{77}$$

In plane configuration, the energy release rate in each mode is translated analytically by the expression (70)

$$G_1(t) = \frac{1}{8} \cdot \left[2 \cdot C_1(t) - C_1(2t) \right] \cdot \left({}^{u}K_1^{(0)} \right)^2 \tag{78}$$

$$G_2(t) = \frac{1}{8} \cdot \left[2 \cdot C_2(t) - C_2(2t) \right] \cdot \left({}^{u}K_2^{(0)} \right)^2 \tag{79}$$

${}^{u}K_1^{(0)}$ and ${}^{u}K_2^{(0)}$ are the instantaneous stress intensity factors in opening and shear mode, respectively, given by an initial finite element calculus. Figure 12 and 13 present the comparison of numerical results of viscoelastic energy release rate given by the $M\theta$ procedure and analytical results resulting of equations (78) and (79) in pure opening mode $\left(\beta = 0^{\circ} \right)$ and pure shear mode $\left(\beta = 90^{\circ} \right)$. Figure 14 and 15 show the same comparison of the energy release rate in mixed mode $\beta = 45^{\circ}$. (${}^{1}G_v$ part of opening mode, ${}^{2}G_v$ part of shear mode). The progression of the energy release rate is given versus time. The results are

calculated by using the crown integration $C6$. We observe a perfect agreement between numerical and analytical results. We note also, in the case of mode I, mode II and mixed, the average error is definitely lower than 1%.

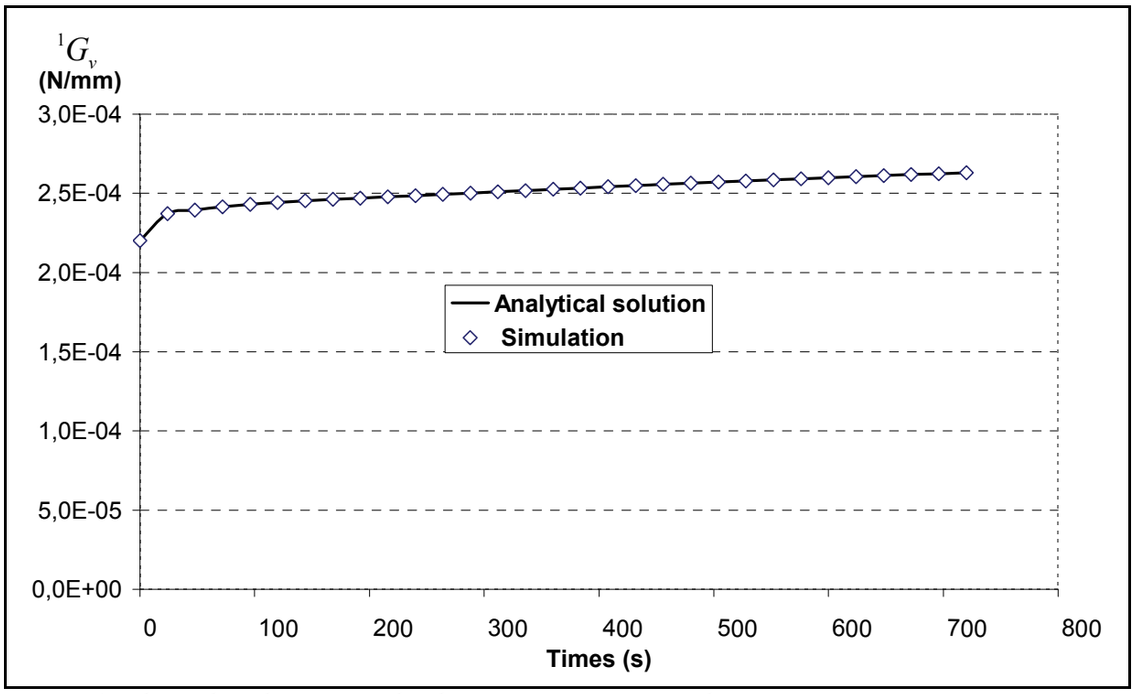

Fig. 12. Analytical and numerical solution in opening mode

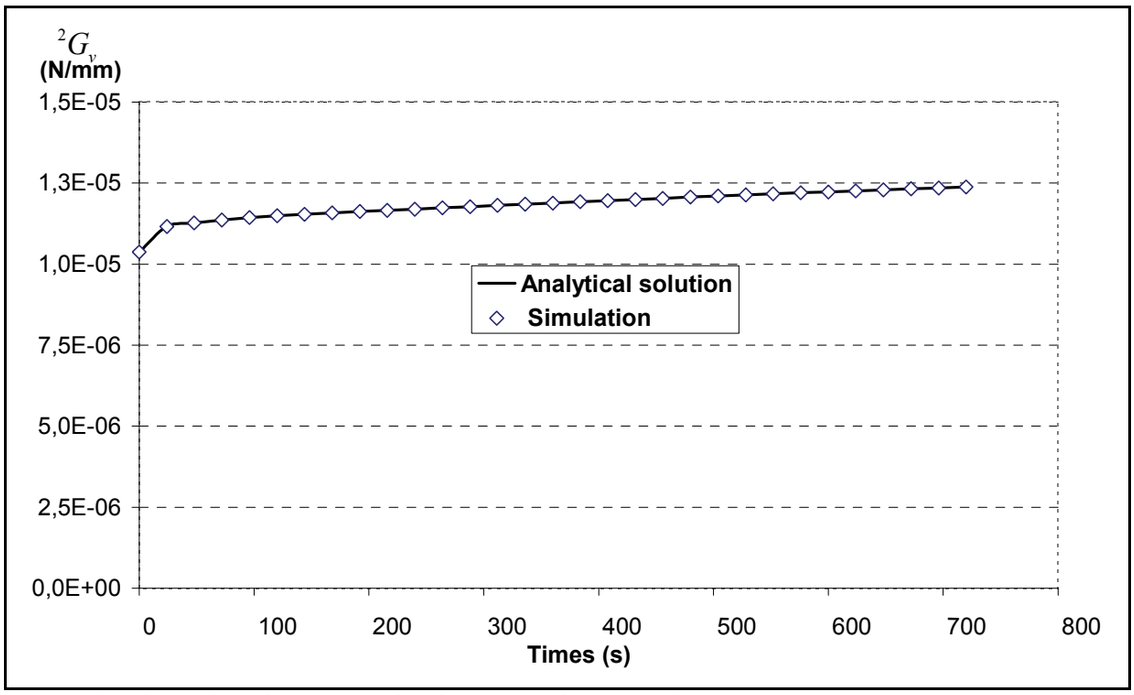

Fig. 13. Analytical and numerical solution in shear mode

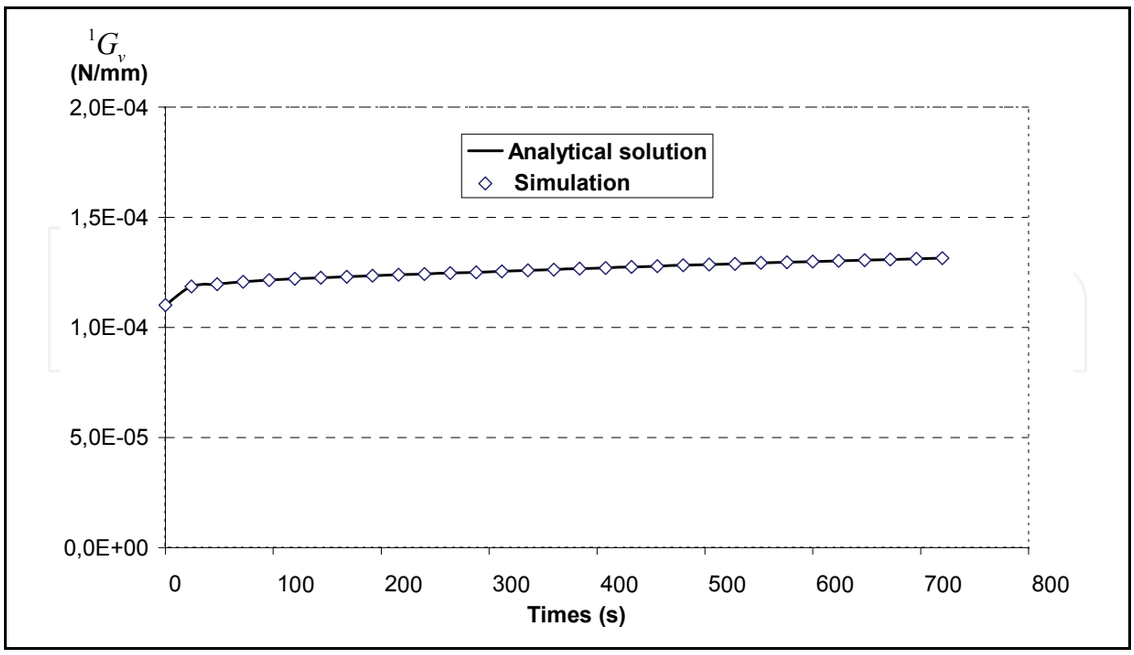

Fig. 14. Analytical and numerical solution in mixed mode (part of opening mode 45°)

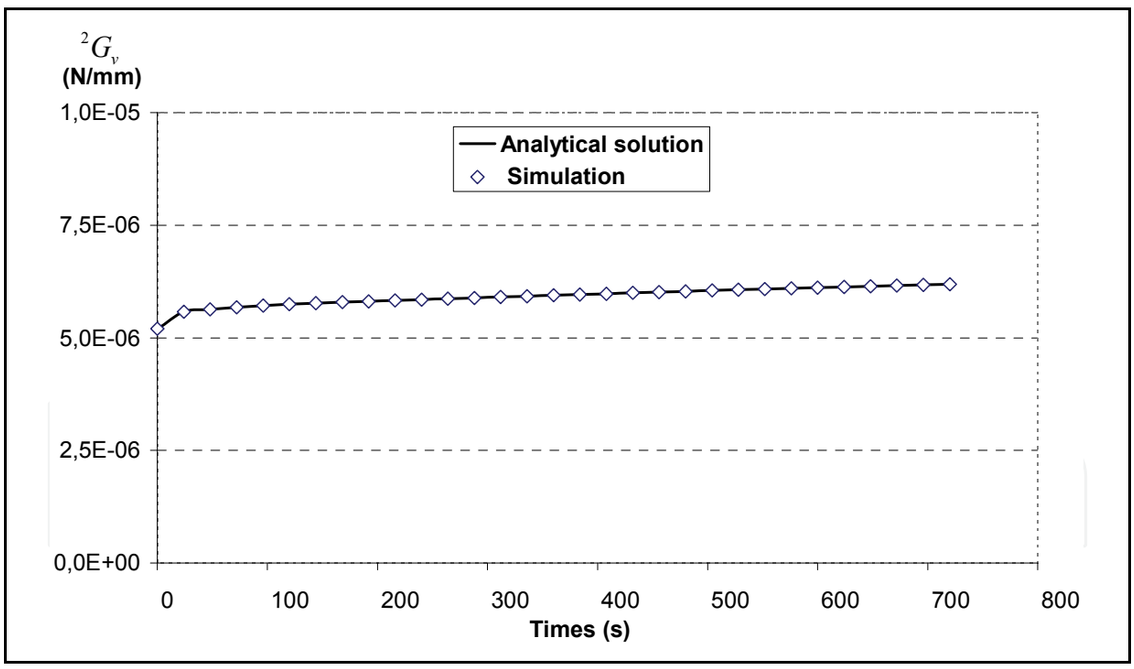

Fig. 15. Analytical and numerical solution in mixed mode (part of shear mode 45°)

7. Conclusion

This chapter has treated the complex problem of the fracture mechanic process in an orthotropic and viscoelastic media. The global algorithm, implemented in the finite element method, is a coupling of viscoelastic subroutine and fracture mechanic tools. According to a

stationary crack, the Mθ-integral is employed in order to compute open and shear parts of energy release rate versus time by taking into account, via the Helmholtz's free energy potential, dissipated and released energy induced by viscoelastic properties.
However, if the crack growth initiation is a high important problem in terms of timber structure design, the problematic of the crack process remains important in the structure live approach taking into account long term behaviours. In this condition, this work leads to be completed in order to integrate the time crack growth process in elements loading by constant or variable loadings.
Finally, timber structures placed in outdoor conditions are subject to climatic variations. In this case, this work must be generalized by introducing moisture variation effect in the crack tip vicinity in the speed increase of crack growth initiation and crack growth proapagation.

8. References

Bui, H.D. & Proix, J.M. (1985). Découplage des modes mixtes de rupture en thermo-élasticité par des intégrales indépendantes du contour. *Actes du Troisième Colloque Tendances Actuelles en Calcul de Structure*, Bastia pp. 631-643.

Bui, H.D (2007) Conservation laws, duality and symmetry loss in solid mechanics. *International Journal of Fracture*, Vol. 147, 163-172.

Chen, F.M.K. and Shield, R.T. (1977). Conservation laws in elasticity of the J-integral type. *Journal of Applied Mechanics and Physics*, Vol. 28, No 1, 1-22.

Chazal, C., & Dubois, F. (2001). A new incremental formulation in the time domain of crack initiation in an orthotropic linearly viscoelastic solid. *Mechanics of Time Dependent Materials*, Vol. 5, 2001, 3-21.

Destuynder, Ph., Djaoua, M. and Lescure, S. (1983). Quelques remarques sur la mécanique de la rupture élastique. *Journal de Mécanique Théorique et Appliquée*, Vol. 2, No 1, 113-135.

Dubois, F. Petit, C. (2005). Modeling of the crack growth initiation in viscoelastic media by the $G\theta_v$-integral. *Engineering Fracture Mechanics*, Vol. 72, 2821-2836.Dubois, F., Chazal, C., Petit, C. (1999) Modeling of crack growth initiation in a linear viscoelastic material. *Journal of Theoritical and Applied Mechanics*, Vol. 37, No 2, 207-222.

Dubois, F., Chazal, C., Petit, C. (2002) Viscoelastic crack growth process in wood timbers: An approach by the finite element method for mode I fracture. *International Journal of Fracture*, Vol. 113, No 4, 367-388.

Ghazlan, G., Caperaa, S. and Petit, C. (1995). An Incremental formulation for the linear analysis of thin viscoelastic structures using generalized variables. *International Journal of Numeric Methods Engineering*, Vol., No 38: 3315-33.

Irwin, G.R. (1957) Analysis of stresses and strains near the and of a crack traversing a plate. *Journal Applied Mechanics*, Vol. 24, 361-385.

Moutou Pitti, R., Dubois, F., Petit, C., Sauvat N (2007) Mixed mode fracture separation in viscoelastic orthotropic media: numerical and analytical approach by the Mθv-integral. *International Journal of Fracture*, Vol. 145, No 3, 181-19, ISSN 0376-9429 (Print) 1573-2673 (Online).

Moutou Pitti, R. (2008). Mixed mode fracture separation in viscoelastic orthotropic materials : modeling and experimentation. Ph.D.thesis, Limoges University . http://www.unilim.fr/theses/2008/sciences/ 2008limo4025/notice.htm. Accessed 23 Jan 2009.

Noether, E. (1971). Invariant variations problem. *Transport Theory and Statistical Physics*, Vol. 1, No 3, 183-207.

Richard, HA. (1981) A new compact shear specimen. *International Journal of Fracture*, Vol. 17, No 5, R105-R107.

Rice, J.R. (1968). A path independent integral and the approximate analysis of strain concentrations by notches and cracks. *Journal of Applied Mechanics*, Vol. 35, 379-386.

Masuero, J.R. & Creus, G.J. (1993) Finite elements analysis of viscoelastic fracture. *International Journal of Fatigue*, Vol. 60, 267-282.

Staverman, A. J., & Schwarzl, P. (1952) Thermodynamics of viscoelastic behavior. *Proceeding Academic Science*, Vol. 55, 474-492.

Valentin, G. & Caumes, P. (1989) Crack propagation in mixed mode in wood: a new specimen. *Wood Science and Technology*, Vol. 23, No 1, 43-53.

Zienkiewicz, O.C., Watson, M., King, I.P. (1968) A numerical method of viscoelastic stress analysis. *Int. J. Mech. Sci*., Vol. 10, 807-827.

Finite Element Analysis

Edited by David Moratal

ISBN 978-953-307-123-7

Hard cover, 688 pages

Publisher Sciyo

Published online 17, August, 2010

Published in print edition August, 2010

Finite element analysis is an engineering method for the numerical analysis of complex structures. This book provides a bird's eye view on this very broad matter through 27 original and innovative research studies exhibiting various investigation directions. Through its chapters the reader will have access to works related to Biomedical Engineering, Materials Engineering, Process Analysis and Civil Engineering. The text is addressed not only to researchers, but also to professional engineers, engineering lecturers and students seeking to gain a better understanding of where Finite Element Analysis stands today.

InTech Europe

University Campus STeP Ri
Slavka Krautzeka 83/A
51000 Rijeka, Croatia
Phone: +385 (51) 770 447
Fax: +385 (51) 686 166
www.intechopen.com

InTech China

Unit 405, Office Block, Hotel Equatorial Shanghai
No.65, Yan An Road (West), Shanghai, 200040, China
中国上海市延安西路65号上海国际贵都大饭店办公楼405单元
Phone: +86-21-62489820
Fax: +86-21-62489821

IntechOpen